Research Square

Preprints are preliminary reports that have not undergone peer review.
They should not be considered conclusive, used to inform clinical practice,
or referenced by the media as validated information.

Synergistic Effects of Sulphur Content and Submerged Arc Welding Parameters on the Mechanical Properties, Corrosion Resistance, and Microstructural Evolution of API 5L X60 Steel

Dr. Haider Mahdi lieth

haider.lieth@uobasrah.edu.iq

University of Basrah

Muslim Qasem Abdulredah

University of Basrah

Research Article

Keywords: API 5L X60 steel, sulphur content, submerged arc welding, corrosion resistance, mechanical properties, microstructure, heat input, FeS

Posted Date: August 20th, 2026

DOI: https://doi.org/10.21203/rs.3.rs-10367871/v1

License: This work is licensed under a Creative Commons Attribution 4.0 International License.
Read Full License

Additional Declarations: No competing interests reported.

Synergistic Effects of Sulphur Content and Submerged Arc Welding Parameters on the Mechanical Properties, Corrosion Resistance, and Microstructural Evolution of API 5L X60 Steel

Muslim Qasem Abdulredah [1]*, Haider Mahdi Lieth[2]

[1]Material Engineering Department, University of Basra, Basra- Iraq.

[2]Mechanical Engineering Department, University of Basra, Basra- Iraq.

E-mail addresses : Muslim.qasemm@uobasrah.edu.iq , Haider.lieth@uobasrah.edu.iq

ABSTRACT

The synergistic impacts of various sulphur concentrations and other factors affecting submerged arc welding (SAW) on the mechanical characteristics, microscopic effects, microevolution, and corrosion resistance of API 5L X60 pipe steel are examined in this study. After creating welded samples with different welding voltage, current, and speed combinations, the samples were exposed to simulated corrosion environments with high and low sulphur contents for 28 days. Weight loss measurements were used to evaluate corrosion behaviour, and scanning electron microscopy (SEM), energy-dispersive X-ray spectroscopy (EDS), and X-ray diffraction (XRD) were used to characterise corrosion products and surface morphology. Tensile and hardness tests were used to assess mechanical performance.

The findings demonstrated a significant correlation between the content of sulphur in the exposure media and corrosion behaviour. In the high-sulfur environment, the average corrosion rate was 0.152 mm/year, but in the low-sulfur environment, it was just 0.019 mm/year, suggesting an eight-fold increase in corrosion severity. Whereas the low-sulfur environment mainly produced a thin oxide-rich layer with no discernible sulphide phases, the high-sulfur environment encouraged the production of a non-protective, porous corrosion layer including iron oxides (Fe_2O_3/Fe_3O_4) and iron sulphide (FeS).With significant sulphur exposure, mechanical degradation was even more noticeable; the ultimate tensile strength dropped from 569 MPa to 506 MPa, and the average yield strength dropped from 534 MPa to 441 MPa.

The corrosion resistance and mechanical performance of the welded joints were improved by increasing the welding speed from 21 to 31 mm/s, which decreased the heat input and further enhanced the grain structure of the weld metal and the heat-affected zone. Overall, the findings show that the long-term performance of API 5L X60 steel is significantly

influenced by the combined impacts of sulfur-induced corrosion and welding-induced micro-changes. Therefore, to increase the longevity and dependability of pipeline steel operating in sulfur-rich environments, it is crucial to improve the parameters of submerged arc welding, particularly welding speed and input heat.
Keywords: API 5L X60 steel; sulphur content; submerged arc welding; corrosion resistance; mechanical properties; microstructure; heat input; FeS.

Keywords: API 5L X60 steel; sulphur content; submerged arc welding; corrosion resistance; mechanical properties; microstructure; heat input; FeS

1. INTRODUCTION

1.1 General Background

Although crude oil is still one of the main sources of world energy, pipelines for its transport are highly susceptible to corrosion (Chougle and Mumbai, 2015). Corrosion is often caused by the reaction of sulfur compounds with iron under higher temperature and the deposition of iron sulfide in pipe inner surface(Meriem-benziane, Bou-saïd and Boudouani, 2017). Crude oil includes sulfur, nitrogen, and oxygen; those with a low sulfur content are classified as "sweet" crude (≤ 0.5 wt% S), while high-sulfur oils are grouped as "sour" [(Oil, no date), (Yasin *et al.*, 2013)]. Sulfur compounds lead to corrosive hydrogen sulfide (H_2S) production during refining and transport (Juhe *et al.*, 2013), which accelerates iron sulfide scale formation. This leads to reduced integrity of the pipeline, pitting over time which in turn may lead to unstable scales formation [(Vetere, Pr and Schrader, 2021),(Goda, Shehata and Gamal, 2019)]. Regarding the abundant reserves of oil in Iraq and the crude oil refineries upgrading, which provide an opportunistic factor for sulfur-induced corrosion to take a deeper understanding of the sulfur affects on API 5L X60 steel is based on a systematic strategic importance [(Saadi, Cherepovitsyn and Semenova, 2022),(Alzahawy and Issa, 2024)].

1.2 API 5L Pipeline Steel

1 API Specification 5L: 2 · Standards for steel line pipe The X grades titles apply to progressively higher classifications of strength; for example PSL 2 defines more rigorous requirements than PSL 1 for demanding operating environments(Segment and Edition, 2004). API 5L X60 is a low-alloy carbon steel widely used in transmission pipelines for its good performance in strength, weldability and cost(Grade, 2026).

1.3 Corrosion Mechanisms in Oil Industry

Corrosion in oil and gas environments is mainly caused by hydrogen sulfide (H_2S), carbon dioxide (CO_2), organic acids and salts triggering mechanisms such as pitting, hydrogen-induced cracking (HIC) or sulfidation(Groysman, 2017). Water with dissolved H_2S and CO_2 percolated onto the steel surface leads to uniform metal loss or localized corrosion pits which represent high risks (Luo, 2020). Corrosion control approaches range from the selection of resistant alloys (especially API 5L X60) and protective coatings to cathodic protection systems, corrosion inhibitors, and regular inspections(Abubaker *et al.*, 2020).

Table 1 Chemical composition analysis

X60	C	MN	P	S	Si	Ni	Cr	Cu	V	Ti
	MAX.	MAX.	MAX.	MAX.	MAX.	MAX.	MAX.	MAX.	MAX.	MAX.
Standard	≤ 0.26%	≤ 1.40%	≤ 0.03%	≤ 0.03%	≤ 0.4%	≤ 0.50%	≤ 0.50%	≤ 0.50%	≤ 0.10%	≤ 0.06%
Actual	0.078	1.39	C<0.003	C<0.002	0.251	0.116	0.013	0.014	0.019	0.015

1.4 Application of Submerged Arc Welding (SAW)

Due to its high deposition rates, stable arc characteristics and deep weld penetration, Submerged Arc Welding (SAW) is widely used for pipeline fabrication. In SAW, a wire electrode that is constantly fed (AW) travels under a blanket of granular flux, which protects the molten weld pool from atmospheric contamination (Operations and Division, 2010). Parameters (e.g. welding current, voltage, travel speed and heat input) which influence the mechanical properties and corrosion resistance of the weld significantly. Finer grain structures in the weld metal and heat-affected zone (HAZ) are achieved with higher welding speeds resulting in lower heat inputs which finally improve mechanical and corrosion performance. On the other hand, excessive heat input coarsens the grains in HAZ and make it more prone to corrosion (Sharma, Rajput and Singh, 2019)(Singh, Singh and Singh, 2020). This is why SAW parameter optimization is necessary to achieve production of sour-service grades with no defects.

1.5 Current Work Objectives

This study investigates the influence of different concentrations of H_2SO_4, which simulates sulfur content in crude oil, on the corrosion performance and tensile properties of welded API 5L X60 steel;

- Assessment of corrosion rates and surface morphology via weight loss, Tafel polarization, scanning electron microscopy (SEM) energy-dispersive X-ray spectroscopy (EDS), and X-ray diffraction (XRD).
- Physical degradation assessment based on tensile testing and hardness measurements.

- Establishing a basis for relationships between microstructural transformations due specifically to oxidation versus sulfide formation and reductions in yield strength, ultimate tensile strength, and ductility(Barros *et al.*, 2016).

- The effect of SAW parameters (voltage, current and welding speed) over corrosion resistance and mechanical performance at high/high concentrations of sulphur content.

2. EXPERIMENTEL WORK

2.1 Base Metal Chemical Analysis

The base metal used in this study is API 5L X60 carbon steel, obtained from local oil companies in Basrah Governorate. Chemical composition analysis was performed according to ASTM A751-14 using a SPECTROTEST TXC25 spectrum analyzer at the University of Basrah. The results confirmed that the material meets API 5L X60 specifications, with actual composition detailed in Table (1) (Lafth and Lieth, 2025).

2.2 Crude Oil Sulfur Content Analysis

New crudes samples were taken from a number of Iraqi refineries in Basra, Samawa, Maysan Najaf and Nasiriyah. X-Ray Fluorescence (XRF) analysis was used to determine sulfur content. Flash point, density and viscosity were some of the other physical properties recorded. Results indicated significant variations of sulfur content in which Samawa crude had the highest value (4.7899 wt%) while Basra crude recorded lowest value (3.0261 wt%). Corrosive solutions used in immersion tests thereafter were prepared on the basis of these two samples(Saadi, Cherepovitsyn and Semenova, 2022) .

2.3 Specimens Preparation

Steel Plates of Measurements 15 cm × 30 cm were used which were cut to smaller specimens as per the test requirements:Immersion test specimens: 5.5 cm × 1 cm × 1 cm (total of 36 specimens)− Tensile test samples: manufactured in accordance with the ASTM E8-E8M specification (54 samples)Microstructural specimens: for SEM, EDS and XRD analysesEach specimen was ground stepwise with emery papers with 200 to 2000 grit, and polished to leave a lustrous smooth surface in compliance of guidelines from the American Society of Testing Materials (ASTM E3)(Coatings, 2017a)(Environments, no date) [22,-25].

2.4 Welded Samples Preparation

The study performed at Al-Shuaiba Refinery in Basra, Iaq, by various welding processes represented by Submerged Arc Welding (SAW). The edges of the steel plate were beveled to provide a suitable weld groove. Three-six welding parameter combinations were utilise employing voltage between 30–35 V; current from 530–590 A and weld speed from 21 to 31 mm/s as well as sample with high or low concentrations of sulphur were welded using the same set of parameters in order ensure homogeneity across specimens.

3. RESULTS AND DISCUSSION

3.1 Preparation of Hostile (Corrosive) Conditions

Based on the sulfur content analysis of crude oil (highest 4.7899 wt% and lowest 3.0261 wt%), two sulfuric acid (H_2SO_4) solutions were prepared using the dilution law ($C_1V_1 = C_2V_2$):

- **High concentration (H-group):** 0.3250 ml H_2SO_4 diluted in 4 liters of distilled water
- **Low concentration (L-group):** 0.2500 ml H_2SO_4 diluted in 4 liters of distilled water

These solutions simulate the corrosive environment caused by sulfur compounds in crude oil. Welded specimens were fully immersed for 4 weeks (28 days) at room temperature. Unimmersed welded specimens were kept as reference samples for comparison.

Table2 . sulfuric acid solution concentrations

Sample Location	Sulfur Content (wt%)	Flash Point (°C)	Density (gm/cm^3 at 15°C)	Viscosity (cSt at 50°C)
Maysan	4.4582	92	0.9699	196
Najaf	4.1454	90	0.9578	150
Nasiriyah	4.4984	118	0.9647	184
Sayni	3.5096	90	0.9412	72
Dura	4.5043	102	0.9611	184
Bazyan	3.9429	118	0.9602	190
Baiji	3.8357	128	0.9564	163
Samawa	4.7899	129	0.9722	318
Kar	3.8352	102	0.9522	123

Kassak	4.0328	100	0.9654	219
Basra	3.0261	< 20	0.8873	13.4
Gayara	3.0302	126	0.9738	226

3.2 Weight Loss Measurements

After thoroughly immersing welded API 5L X60 specimens for 28 days in its two sulfuric acid solutions of different concentrations (H-group: high concentration [0.3250 ml H_2SO_4 per 4 L distilled water], and L-group: low concentration [0.2500 ml H2 SO4 per 4 L distilled water]), weight loss measurements were performed. Corrosion rate (CR) was calculated according to the following equation(Environments, 1999):

$$CR\ (mm/y) = A \times T \times DK \times W$$

where:

Constant: (K = 8.76 \times 10^4)

(W) = weight loss (g),

A = exposed surface area (cm^2),

(T) = exposure time (hours),

Net density of steel(g/cm^3): (D)

Table3 The corrosion rate and weight loss for High Sulphur Concentration API 5L (X60) .

Sample	Media	NO.	Weights (g)					WΔ	CR (mm/y)
			Original	After immersion					
				1 Week	2 Week	3 Week	4 Week		
X60	S1	1	42.2843	42.271	42.2461	42.2442	42.233	0.0513	0.118
		2	43.78	43.765	43.753	43.7398	43.7134	0.0666	0.152
		3	43.008	42.9838	42.9741	42.9669	42.9434	0.0646	0.148
		4	41.2903	41.2799	41.2646	41.2554	41.2363	0.054	0.124
		5	43.3768	43.3455	43.3262	43.3189	43.307	0.0698	0.16
		6	43.4788	43.465	43.4504	43.4447	43.4257	0.0531	0.122
		7	41.7607	41.7478	41.735	41.725	41.7008	0.0599	0.137
		8	42.5694	42.5534	42.5423	42.5307	42.5137	0.0557	0.128
		9	42.6787	42.6693	42.6605	42.6521	42.6288	0.0499	0.114
		10	42.6383	42.6235	42.6129	42.5942	42.5795	0.0588	0.135
		11	43.5969	43.5738	43.5613	43.5353	43.5275	0.0694	0.159
		12	43.0083	42.993	42.9903	42.972	42.9503	0.058	0.133
		13	46.5383	46.5031	46.482	46.453	46.4337	0.1046	0.239
		14	46.2995	46.2778	46.253	46.2377	46.2281	0.0714	0.164
		15	44.9369	44.9148	44.8931	44.8814	44.8735	0.0634	0.145
		16	42.3421	42.3159	42.2927	42.2807	42.2707	0.0714	0.164
		17	45.318	45.2878	45.263	45.2463	45.2407	0.0773	0.177
		18	45.7721	45.7449	45.7238	45.7113	45.711	0.0611	0.14

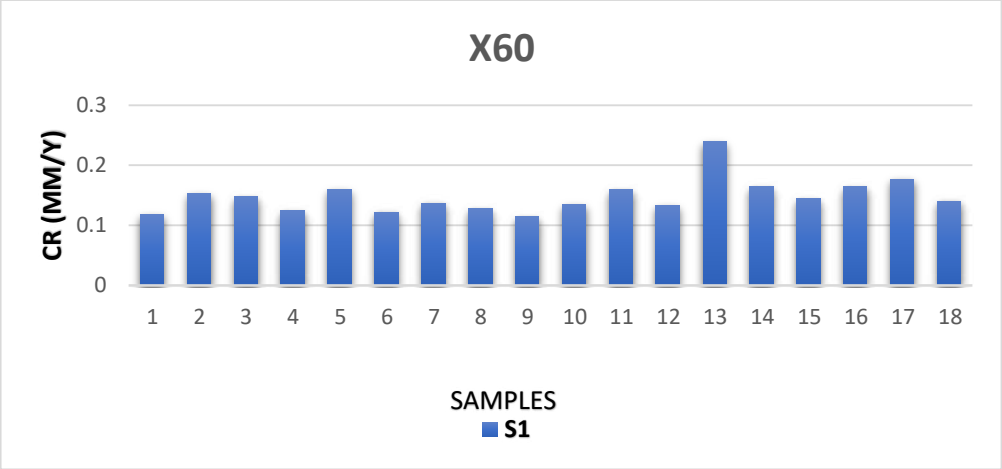


Fig 1 .corrosion rate for API X60 for High concentration solution

Table 4 . The corrosion rate and weight loss for Low Sulphur Concentration API 5L (X60) .

Sample	Media	NO.	Weights (g)					WΔ	CR (mm/y)
			Original	After immersion					
				1 Week	2 Week	3 Week	4 Week		
X60	S2	1	43.2135	43.2031	43.181	43.1739	43.143	0.0705	0.0212
		2	43.1213	43.1061	43.0835	43.9746	43.0541	0.0672	0.0202
		3	43.3351	43.3205	43.3014	43.2902	43.2643	0.0708	0.0213
		4	43.1788	43.1634	43.137	43.1343	43.1128	0.066	0.0198
		5	40.9658	40.9432	40.929	40.9209	40.9022	0.0636	0.0191
		6	41.5318	41.5181	41.4982	41.4892	41.467	0.0648	0.0195
		7	41.971	41.9445	41.9288	41.9221	41.9047	0.0663	0.0199
		8	42.2608	42.2463	42.2259	42.2207	42.1957	0.0651	0.0196
		9	42.4257	42.4056	42.3872	42.375	42.3596	0.0661	0.0199
		10	43.5364	43.5228	43.505	43.4999	43.4766	0.0598	0.018

		11	42.6893	42.6724	42.6527	42.6445	42.622	0.0673	0.0202
		12	44.6085	44.5998	44.5749	44.5648	44.5454	0.0631	0.019
		13	40.1586	40.1484	40.1279	40.118	40.0977	0.0609	0.0183
		14	46.2315	46.2094	46.187	46.1773	46.1582	0.0733	0.022
		15	45.8455	45.8258	45.8007	45.7945	45.776	0.0695	0.0209
		16	43.535	43.5271	43.4849	43.481	43.461	0.074	0.0223
		17	41.4958	41.4951	41.4772	41.4675	41.456	0.0398	0.012
		18	42.9233	42.9038	42.8879	42.8772	42.8571	0.0662	0.0199

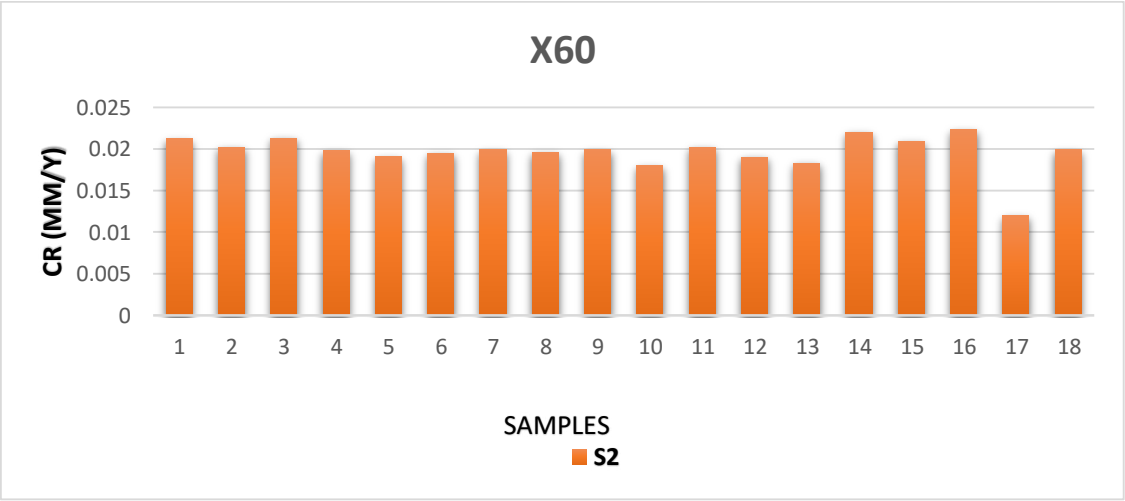


Fig 2.corrosion rate for API X60 for low concentration solution

Results in terms of weight loss demonstrated a dependence on the H_2SO_4 concentration. The corrosion rate was measured from H-group (high concentration) varied from 0.114 to 0.239 mm/y with an average of around 0.152 mm/y as shown in Fig.S4(b) and the weight loss is represented in Table S2, Sample H13 has registered a maximum weight loss (0.1046 g) and corrosion rate (0.239 mm/y). The corrosion rate in the L-group (low concentration) varied between 0.012 and 0.0223 mm/y, with an average value of around 0.019 mm/y; sample L17 had in turn the lowest weight loss (0.0398 g) and corrosion rate (0.012 mm/y).Results of the exposed welded API 5L X60 steel steels revealed that H-corrosion rate in the average was about an order of decade measurements H-group, which did support that higher level of concentrations of H_2SO_4 beneficially quickens the corrosion

attack on welded API 5L X60 by a number of orders. The formation of non-protective mixed iron oxide and iron sulfide layers in high-concentration environments (SEM/EDS) as opposed to the thin, protective oxide films developed under low-concentration environment leads to this result. Corrosion rates of API 5L X60 welded specimens immersed for four weeks in high and low H_2SO_4 concentrations are also summarized in Tables (3) and Figure (1). The corrosion rates for the H-group (high concentration) were in the range between 0.114 and 0.239 mm/y (average value 0.152 mm/y), as for L-group (low concentration) they were much lower, ranging from 0.012 to 0.0223 mm/y (average value 0.019 mm/y). The average corrosion rate in the H-group was roughly ten times that of the L-group, suggesting that increased sulfur content (simulated by H_2SO_4 concentration) greatly enhances degradation of materials(Burhagohain, Sharma and Malla, 2022). This observation is consistent with microstructural results, in which H-group samples exhibited non-protective mixed oxide-sulfide layers and L-group was shown to only form thin oxide films with protective nature.

3.4 Microstructure Analysis

Scanning Electron Microscope (SEM) is a high magnification tool for surface morphology and microstructure studies. The topography is revealed in clear detail, including grains, boundaries, cracks, pits and porosity. To be effective at imaging, SEM requires samples to be conductive or have a coating of gold/carbon on non-conductive materials. In addition to SEM, Energy Dispersive X-ray Spectroscopy (EDS) is an analytical technique that identifies elemental composition qualitatively and semi-quantitatively. This is achieved by means of point analysis, line scanning, and elemental mapping that may see corrosion products and alloying elements but lacks sensitivity to lighter elements. X-ray Diffraction (XRD) is furthermore a non-destructive method used to give information about crystalline phases in a certain sample. It can identify specific compounds, like iron carbonate ($FeCO_3$) from CO_2 corrosion or iron sulfide (FeS) from H_2S corrosion(Groysman, 2017). This tool also allows us for the semi-quantitative phase analysis and gives information about the crystallite size.

As previously mentioned, three samples immersed in high concentration and three others in low concentration were examined, in addition to the analysis of non-immersed samples for comparative purposes, as well as the metal as cast. Furthermore, the corrosion residues collected from the high and low concentration solutions were also analyzed. EDS, SEM, and XRD examinations were conducted(Press, 1998).

Table 5 **. Distribution of tested samples for SEM, EDS, and XRD analyses**

TEST	SAMPLE	IMMERSED		NON IMMERSED
		HIGH CON.	LOW CON.	
SEM	AS CAST	1,9	10,12	10,12
EDS	AS CAST	1,9	10,12	10 ,12
XRD	AS CAST	1,9	10,12	10, 12

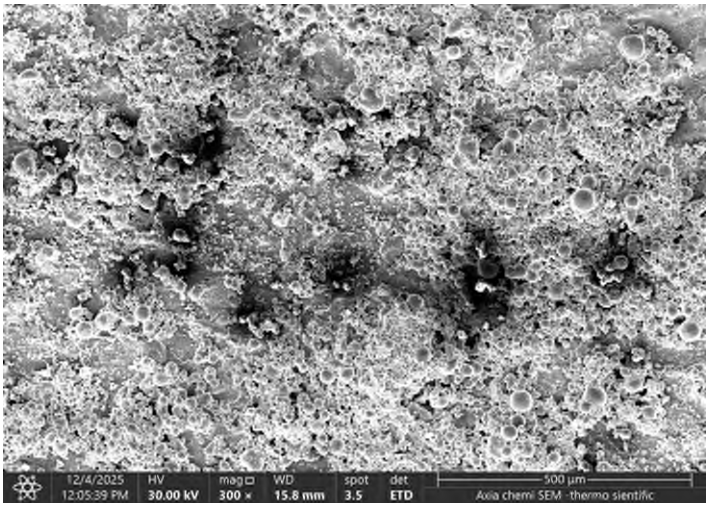


Fig 3. Sample AS CAST (500 µm) SEM

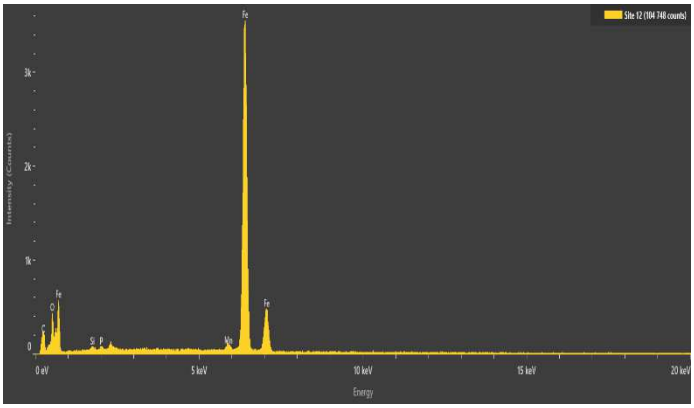


Fig 4.EDS TEST TO BASIC METAL SAMPLE

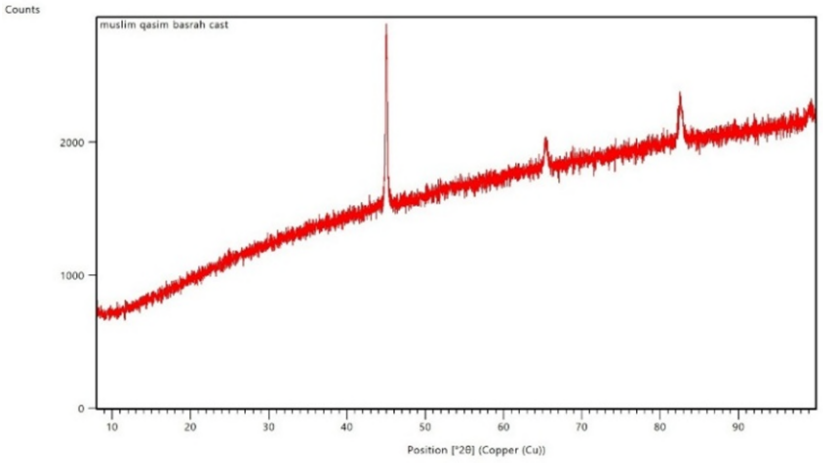


Fig 5. XRD TEST TO BASIC METAL SAMPLE

The scanning electron microscope (SEM) micrographs are observed at different magnificences from 300× to 10,000×, which confirm the topography of a base metal detected in API 5L X60 forms with no welding or corrosion exposure. At the lower magnifications (300× to 600×), the surface appears smooth and homogeneous, disclosing fine parallel grinding or rolling marks representative of the as-manufactured condition, and presents no indication of corrosion products, pitting or irregular deposits. At intermediate magnifications (1,300×-2,500×), the surface retains a more homogeneous appearance and consists only of minor fine particulates from sample preparation and shows no signs of oxidation nor contamination that are beyond a native air-formed oxide film. No acicular structures, porous layers, sulfide phases or corrosion-related features are observed at higher power (5,000× to 10,000×) which further confirms the absence of corrosion attack. This is confirmed from energy dispersive spectroscopy (EDS) analyses where iron (Fe) is determined as the main element however the traces elements are normally associated with API 5L X60 steel. Notably, sulfur (S) is not detected, further corroborating the absence of sulfides. Each XRD pattern consists of narrow and intense peaks that are typical for body-centered cubic (BCC) ferritic iron in a low-carbon steel, with no observable significant peaks from oxides or sulfides confirming that the surface is clean and unreacted. This base metal sample is important to reference for the effects of welding only (not immersed welded samples) and the combined effects of welding and exposure to H_2SO_4 (immersed samples). The differences in microstructure or composition identified in the welded or exposed specimens can now clearly be assigned to either the weld process or to exposure in this corrosive medium(Coatings, 2017b).

3.5 SEM Test

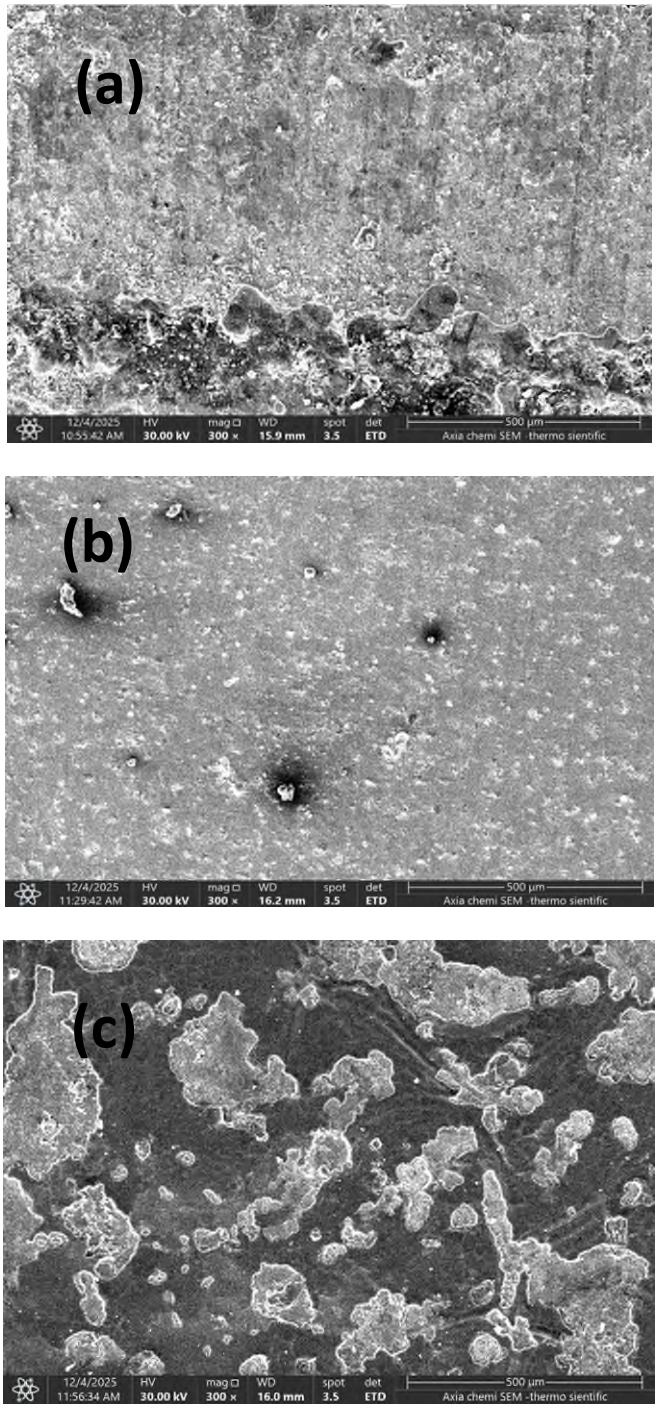


Fig 6. SEM for (a) high concentration (b) low concentration (c) non immersed

3.6 EDS TEST

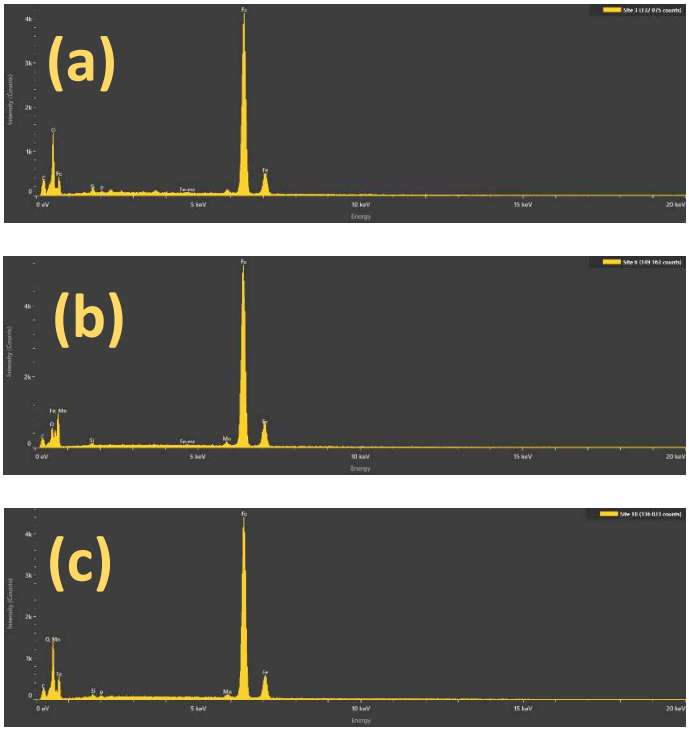
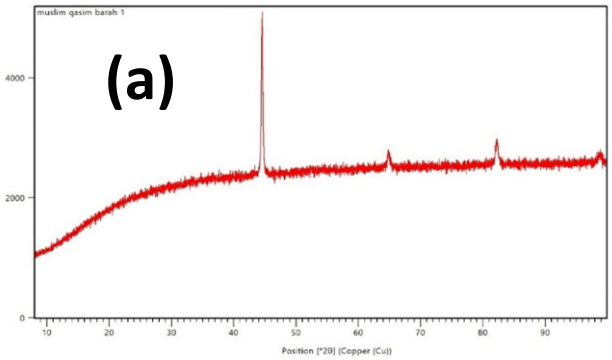


Fig 7. EDS for (a) high concentration (b) low concentration (c) non immersed

3.7 XRD Test



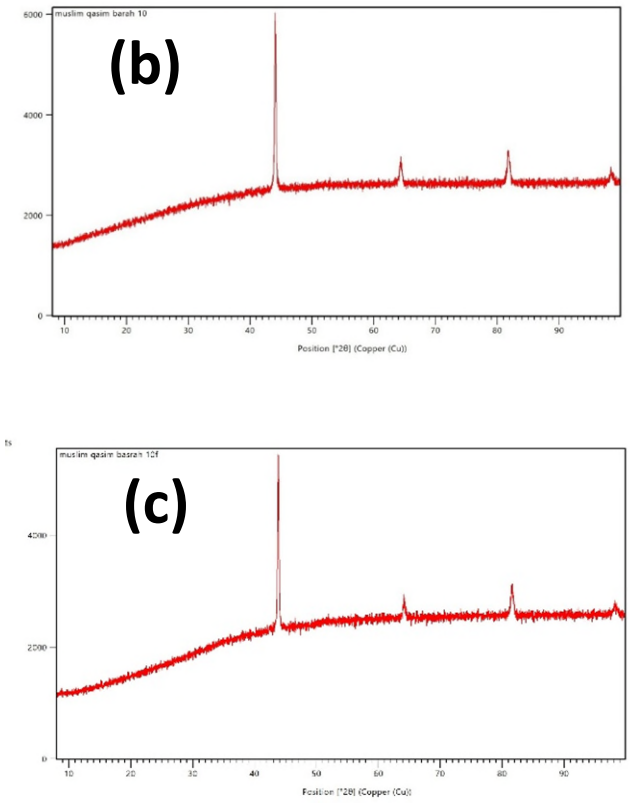
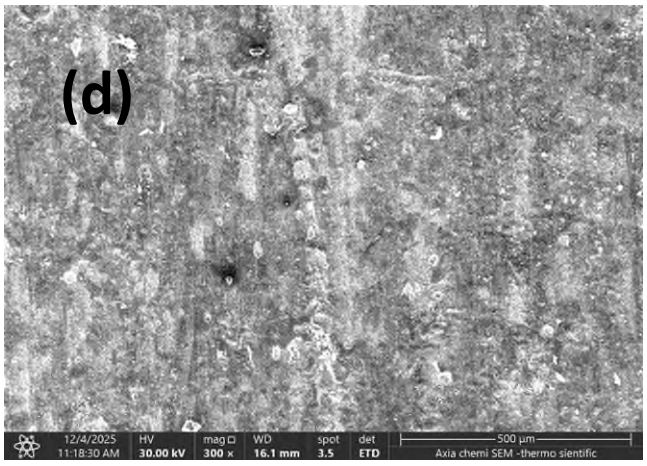
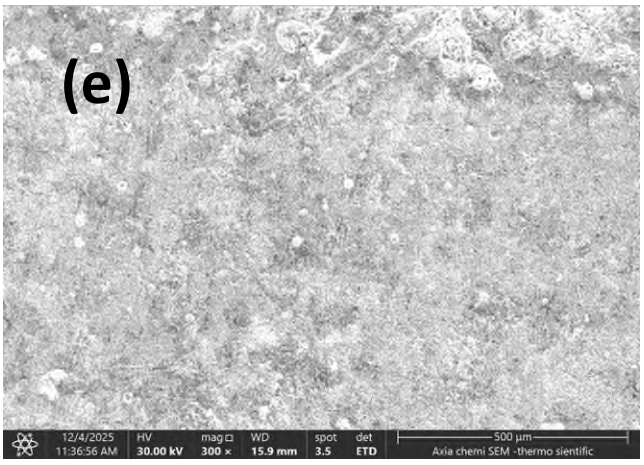


Fig 8. XRD for (a) high concentration (b) low concentration (c) non immersed

H1 (High Absorption): SEM micrographs show a rough and irregular surface which is fully covered by corrosion products. High-magnification image (10,000×) of an individual blade fiber shows acicular (needle-like) structures consistent with a mixed iron oxide and iron sulfide formation. EDS analysis for S at 2.5 keV along with O and Fe (with corresponding peaks) provides confirmation of the presence of sulfur (S), supporting formation of FeS in addition to Fe_2O_3 and Fe_3O_4. XRD patterns show resolute iron peaks, distinct oxide peaks and small sulfide peaks further confirming the formation of a mixed, non-protective corrosion layer.SEM Images from Coprecipitated Samples L10 (Low Concentration) Typically, the surface appears relatively smooth or rough and with only a few small corrosion nodules. There are no acicular structures or extensive pitting. EDS shows no sulfur therefore, it is not subject to sulfidation. We find only trace amounts of oxygen (indicating the presence of a thin,passivating iron oxide layer). XRD shows metallic iron being the dominant oxygenated phase, and oxide peaks quite weakly as well so no evident sulfide peaks.Sample Ref10: SEM image of the unimmersed reference showing a clean welded surface free from any corrosion products but with slight thermal oxidation due to the welding process("Revue Roumaine de Chimie CORROSION INHIBITION OF API5L X60 STEEL IN SULFURIC ACID USING GUM ARABIC," 2023). EDS shows no sulfur and only a

trace amount of oxygen. XRD shows only sharp peaks for metallic iron, indicating no substantial corrosion.Sulfur causes presence in H1 gives a coarse, non-protective oxide–sulfide layer leading to speedy corrosion. On the other hand, the lack of sulfur in L10 and Ref10 leads either to a thin, passivating oxide layer (L10) or even absence of corrosion layer (Ref10), providing superior maintenance of surface integrity and mechanical properties(Cullity and Stock, 2001).





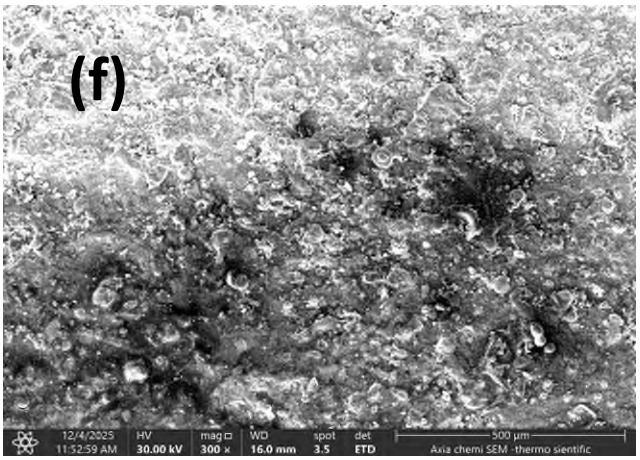


Fig 9. SEM for (d)high concentration (e) low concentration (f) non immersed .

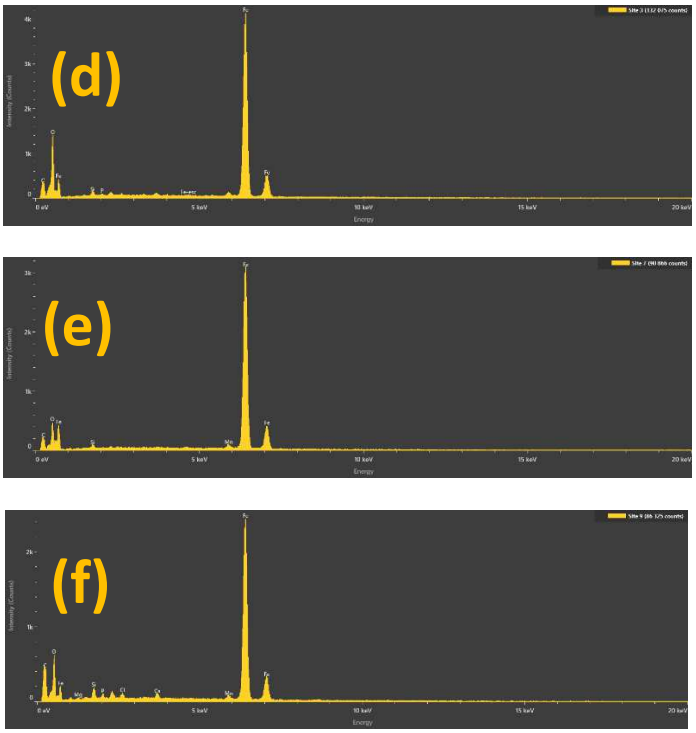


Fig 10. EDS for (d)high concentration (e) low concentration (f) non immersed

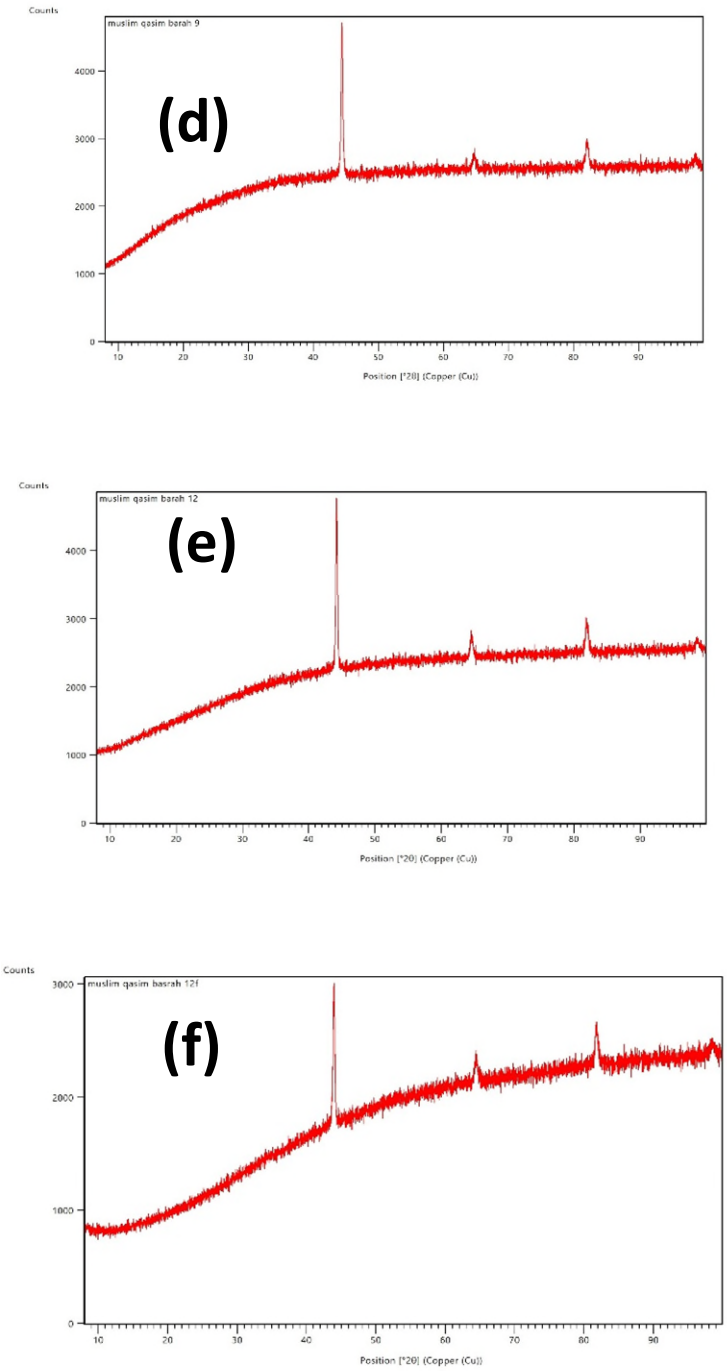


Fig 11. XRD for (d)high concentration (e) low concentration (f) non immersed

Sample H9 (High Concentration) The SEM micrographs show a rough surface covered by irregularly distributed corrosion products, but the degree of attack is much lower than Sample H1 under corresponding conditions due to higher welding speed (31 mm/s instead of 21 mm/s). No acicular structures are detected. Although S is detected at 2.5 keV in EDS

analysis, there is less intensity than at H1 showing lower sulfidation (Fig.11). The XRD patterns also show well defined iron peaks and distinct oxide peaks with weak or absent sulfide peaks, indicating that oxides are dominant over sulfides. This increase in welding speed leads to a reduction in heat input, which refines the grain structure of both the weld metal and HAZ, improving corrosion resistance compared with H1.L12 (Low Concentration) Sample – SEM images showing a reasonably smooth surface with sparse, small corrosion nodules without extensive pitting With the metallic shine of the surface hardly affected. No sulfur is detected by EDS, indicating a lack of sulfidation—only trace oxygen is noted as well, suggesting that the specimen developed a very thin iron oxide protective layer. The dominant phase appears to be metallic iron, corroborated by a minimal presence of oxide peaks (very weak) and no detectable sulfide peaks using XRD standard analysis (see Fig21(Singh and Singh, 2020).Sample Ref12 (Unimmersed Reference): SEM observation of the welded surface showed no corrosion products, but minor thermal oxidation from the welding process. Almost no oxygen and no sulfur found by EDS(Altuntaş *et al.*, 2024). XRD spectra show only sharp metallic iron peaks proving absence of significant corrosion.Seeing as Sample H9 was welded at a much faster gas speed (31 mm/s) than H1 and therefore exhibits a finer microstructure, it is not surprising that the corrosion resistance of sample H9 is higher. However, the sulfide species remains, giving rise to a mixed oxide-sulfide layer and this time less represented than in H1(Calik, Ucar and Semercý, 2024). In comparison, Sample L12 is just gently oxidised with no signs of sulfidation while Ref12 shows no corrosion at all. The effects of increasing welding speed as leading to lower heat input have been shown by these findings which increase the corrosion resistance of welded API 5L X60 steel in both high and low concentration H_2SO_4 environment(Khamees, 2025).

3.8 Effect of Welding Parameters and Sulphur Media on Corrosion and Mechanical Properties

The results strongly show that either welding parameters or environments containing different amount of sulphur can significantly influence corrosion behaviour and mechanical property on API 5L X60 steel. The effects of the welding parameters can be linked to their direct impact on heat input, cooling rate, grain size and distribution in the weld metal and HAZ. The increase from 21 mm/s to 31 mm/s in speed caused heat input per unit length to decrease, resulting in a finer ferritic microstructure and narrower HAZ. Furthermore, it is already known that grain refinement has a positive effect on mechanical properties and corrosion resistance (Choi *et al.*, 2026) because finer grains enhance the boundary density which favours the formation of more homogeneous and cohesive inert layers, while reducing localised galvanic variations in the microstructure. Higher exposure speed indicates lower resistance to corrosion and retention of mechanical properties of the samples that are welded(Zhao *et al.*, 2022).

The high and visible degradation in low-sulphur environments is also attributed to the electrochemical activity of sulphur compounds. As demonstrated before, in a high-sulphur medium corrosion rate measured was approximately eight times higher than in low-sulphur medium, proving that sulphur compounds promote the anodic dissolution of the steel surface to thje great extent. SEM, EDS and XRD examinations suggested the formation of ternary corrosion products such as Fe_2O_3, Fe_3O_4, and FeS(Nnoka, Jack and Szpunar, 2024) .While iron sulphide layers can protect under certain conditions, the solubility of some corrosion products formed in this study were porous, discontinuous, and weakly bound, allowing for replenishment of oxidized ions to be released into solution and exacerbate further corrosion.

Microstructural changes and the formation of soft corrosion products are closely related to the effects on mechanical properties, especially a reduction in yield strength, ultimate tensile strength and hardness due to exposure to sulphur solutions . The ultimate tensile strength decreased from 569 MPa to 506 MPa after being exposed to a high-sulphur medium, while the mean yield strength went down from 534 MPa in the unexposed condition to 441 MPa. These reductions demonstrate that evaporated damage is not limited to just impact and surface material loss but also altered the welded joints load-bearing properties. In addition, localised corrosion defects and iron sulphide phases were probably served as stress concentration sites, which lead to cracks under tensile loading. This interpretation is confirmed by the reduction of the hardness values in the weld metal and heat-affected zone as a function of exposure time, which point toward an incipient microstructure degradation after prolonged testing(Vetere, Pr and Schrader, 2021).

The synergistic effect of welding-induced microstructural heterogeneity and sulphur-related corrosion is one of the most important findings in this study. The weld metal, heat-affected zone and base metal ultimate strength of the parent material change with gains sizes dislocation densities under corrosive conditions leading to localised electrochemical cells]. Such microstructural differences may be amplified in high-sulphur environments due to preferential sulphide production and selective dissolution. Thus, it follows that corrosion is determined by the chemical aggressiveness of the environment as well as the metallic state created by welding (Kermani and Morshed, 2003).This findingunderscores the need for optimisation of welding parameters to minimise microstructural variabilityand provide improved resistance to service conditions in sulphurous environments.

In summary, the results indicate that the mechanical property and corrosion property of API 5L X60 steel are determined by the combination between welding heat input and sulphur contents. Higher welding speeds, which produce finer microstructures and reduces heat input, can mitigate some of the detrimental effects in sulphur-rich environments. Hence, for long-term dependability of pipeline systems under sour crude oil service conditions, careful control of SAW parameters is essential in addition to appropriate material selection and corrosion counter-measure programs (Ahmad, 2024).

4. CONCLUSION

1. Corrosion rate: as the average corrosion rate in the high-concentration H-group (0.152 mm/y) was almost ten times higher than that of low-concentration L-group (0.019 mm/y), it proved that higher concentration of H_2SO_4 significantly enhanced material performance degradation ability.
2. Corrosion products (SEM/EDS/XRD): Their concentration (H-group) led to formation of non-protective mixed layer consisting of iron oxides (Fe_2O_3/Fe_3O_4) and iron sulfides (FeS). The specific layer showed acicular and porous morphology with sulfur peaks easily seen using EDS analysis. In stark contrast, the low-concentration exposure (L-group) produced a mere monolayer of oxidised iron coating with no sulfide phase being detected.
3. Sulfidation Impact: The formation of iron sulfides (FeS) is intimately associated with an increase in corrosion rates, surface roughness and non-protective corrosion layers. On the other hand, oxide-only films maintain surface integrity and are accompanied by reduced corrosion rates.
4. Welding Parameters Effect: Increasing welding speed from 21 mm/s to 31 mm/s decreased heat input, improved grain size in the weld and heat-affected zone (HAZ) and corrosion resistance at this higher welding speed under similar H_2SO_4 test conditions.
5. Corrosion Residues: The H-group corrosion products primarily comprised iron oxides (57.6 at% O; 1.0 at% S) containing low sulfide content, while the L-group residues were insignificant The latter indicates that the oxide-rich corrosion products are more spall-prone than sulfide-dominated ones.
6. Comparisons of Passivation Contributions to Corrosion Performance: Base Metal versus Welded Samples As-Received base metal featured an unblemished, smooth surface and no observable corrosion products on the weld reference samples not exposed to immersion (drier). These findings validate that all scour found resulted from H_2SO_4 exposure instead of welding processes or atmospheric oxidation.

5. RECMMENDATION

This study indicates that grain refinement and corrosion resistance in sour media can be achieved by using relatively high welding speeds (≥31 mm/s) together with low heat input. Internal lining/coating or corrosion inhibitors should be considered for pipelines transporting high-sulfur crude oil in order to prevent sulfidation attack. In particular, it is recommended to perform routine corrosion monitoring of coupons by weight loss and Tafel polarization methods for early diagnosis of degradation. Further research is needed on longer immersion periods, the effect of combined H_2S and CO_2, high temperature effects, and post-weld heat treatment.

6. REFERENCE

Abubaker, I. et al. 2020 “Corrosion Strategy in Oil Field System,” 2(1), pp. 28–39. Available at:https://doi.org/10.33945/SAMI/JCR.2020.1.2.

Ahmad, K. 2024 “Department of mechanical engineering university of engineering and technology peshawar, pakistan,” (May).

Altuntaş, O. *et al.* 2024 “Microstructural, mechanical and nondestructive characterization of X60 grade steel pipes welded by different processes,” *Materials Testing*, 66, pp. 1528–1538. Available at: https://doi.org/10.1515/mt-2024-0121.

Alzahawy, A. and Issa, H. 2024 “The Iraqi Petroleum Refining Industry : A Review of Environmental Impact Assessment The Iraqi Petroleum Refining Industry : A Review of.” Available at: https://doi.org/10.20944/preprints202405.0901.v1.

Barros, I.B. De *et al.* 2016 “The inhibitory action of Bauhinia purpurea extracts on the corrosion of carbon steel in sulfuric acid medium,” 19(1), pp. 187–194.

Burhagohain, P., Sharma, G. and Malla, P. 2022 “Investigation of a few oxazolone molecules as corrosion inhibitor for,” *Egyptian Journal of Petroleum*, 31(3), pp. 37–45. Available at: https://doi.org/10.1016/j.ejpe.2022.06.006.

Calik, A., Ucar, nazım and Semercý, A. 2024 “Mechanical Properties of Welded Joints of Pipeline Steels Joined by Submerged Arc Welding,” *Metal Science and Heat Treatment*, 66. Available at: https://doi.org/10.1007/s11041-024-01069-3.

Choi, Y. *et al.* 2026 “Effect of H 2 S on the Corrosion Behavior of Pipeline Steels in Supercritical and Liquid CO 2 Environments,” 72(8), pp. 999–1009.

Chougle, S. and Mumbai, N. 2015 “Generations of Crude Oil 1,2,” pp. 309–313.

Coatings, S. 2017a “Standard Guide for Preparation of Metallographic Specimens 1,” 11(Reapproved), pp. 1–4. Available at: https://doi.org/10.1520/E0003-11R17.1.

Coatings, S. 2017b “Standard Guide for Preparation of Metallographic Specimens 1,” i(Reapproved). Available at: https://doi.org/10.1520/E0003-11R17.1.

Cullity, B.D. and Stock, S.R. 2001 *Elements of X-ray Diffraction*. Prentice Hall. Available at: https://books.google.iq/books?id=YA03PQAACAAJ.

Environments, C.A. 1999 “Standard Practice for Preparing , Cleaning , and Evaluating Corrosion Test,” 90(Reapproved).

Environments, C.A. “Standard Practice for Preparing , Cleaning , and Evaluating Corrosion Test,” pp. 1–9. Available at: https://doi.org/10.1520/G0001-03.2.

Goda, E.S., Shehata, A.B. and Gamal, H. 2019 “Critical Reviews in Analytical Chemistry Critical Review on the Analytical Methods for the Determination of Sulfur and Trace Elements in Crude Oil Critical Review on the Analytical Methods for the Determination of Sulfur and Trace Elements in Crude Oil,” *Critical Reviews in Analytical Chemistry*, 0(0), pp. 1–18. Available at: https://doi.org/10.1080/10408347.2019.1599278.

Grade, S. (no date) “API 5L Pipe Specification (PSL1 , PSL2 , SOUR SERVICE).”

Groysman, A. 2017 “Corrosion problems and solutions in oil , gas , refining and petrochemical industry Korozní problémy při zpracování plynu a ropy,” pp. 100–117. Available at: https://doi.org/10.1515/kom-2017-0013.

Juhe, Z. *et al.* 2013 “Crude-oil hydrocarbon composition characteristics and oil viscosity prediction in the northern Songliao Basin.” Available at: https://doi.org/10.1007/s11430-013-4656-8.

Kermani, M.B. and Morshed, A. 2003 “Carbon Dioxide Corrosion in Oil and Gas Production — A Compendium,” 59(8), pp. 659–683.

Khamees, L.A. 2025 “Journal of Chemical and Petroleum Engineering (JChPE) A Review of Improving the Heavy Crude Oil Transportation Process Using Additives,” 59(2), pp. 291–338. Available at: https://doi.org/10.22059/jchpe.2025.390285.1596.

Lafth, M.Y. and Lieth, H.M. 2025 “Impact the sulphur content in Iraqi crude oil on the mechanical properties and corrosion behaviour of carbon steel in various types of API 5L pipelines and ASTM 106 grade B.”

Luo, F. 2020 “Study on Corrosion Law of Large Crude Oil Storage Tank Floor and Risk-Based Inspection and Maintenance Technology,” 19(2), pp. 66–74.

Meriem-benziane, M., Bou-saïd, B. and Boudouani, N. 2017 “SC,” *Journal of Petroleum Science and Engineering* [Preprint]. Available at: https://doi.org/10.1016/j.petrol.2017.08.073.

Nnoka, M., Jack, T.A. and Szpunar, J. 2024 “Effects of different microstructural parameters on the corrosion and cracking resistance of pipeline steels : A review,” *Engineering Failure Analysis*, 159(February), p. 108065. Available at: https://doi.org/10.1016/j.engfailanal.2024.108065.

Oil, C. 2018 “CRUDE OIL PETROLEUM.”

Operations, P.E. and Division, D. “Development of Vertical Submerged Arc Welding Method for Aboveground LNG Storage Tank Construction,” 4, pp. 55–62.

Press, P. 2017 “Standard Guide for Quantitative Analysis by Energy-Dispersive Spectroscopy 1,” pp. 1–8.

“Revue Roumaine de Chimie CORROSION INHIBITION OF API5L X60 STEEL IN SULFURIC ACID USING GUM ARABIC” (2023), 68, pp. 17–25. Available at: https://doi.org/10.33224/rrch.2023.68.1-2.02.

Saadi, T.A.L., Cherepovitsyn, A. and Semenova, T. 2022 “Iraq Oil Industry Infrastructure Development in the Conditions of the Global Economy Turbulence.”

Segment, U. and Edition, F. 2004 “Specification for Line Pipe,” (October).

Sharma, H., Rajput, B. and Singh, R.P. 2019 “A review paper on effect of input welding process parameters on structure and properties of weld in submerged arc welding process,” *Materials Today: Proceedings*, 26(xxxx), pp. 1931–1935. Available at: https://doi.org/10.1016/j.matpr.2020.02.422.

Singh, A. and Singh, R.P. 2020 “Materials Today : Proceedings A review of effect of welding parameters on the mechanical properties of weld in submerged arc welding process,” *Materials Today: Proceedings*, (xxxx), pp. 2–5. Available at: https://doi.org/10.1016/j.matpr.2020.02.361.

Singh, R.P., Singh, Aman and Singh, Amit 2020 “Materials Today : Proceedings Optimization of hardness of weld in submerged arc welding,” *Materials Today: Proceedings*, (xxxx), pp. 6–9. Available at: https://doi.org/10.1016/j.matpr.2020.02.382.

Vetere, A., Pr, D. and Schrader, W. 2021 “Qualitative and Quantitative Evaluation of Sulfur-Containing Compound Types in Heavy Crude Oil and Its Fractions.” Available at: https://doi.org/10.1021/acs.energyfuels.1c00491.

Yasin, G. *et al.* 2013 “Quality and chemistry of crude oils,” 4(March), pp. 53–63. Available at: https://doi.org/10.5897/JPTAF12.025.

Zhao, W. *et al.* 2022 “Effect of Heat Input on Microstructure and Corrosion Resistance of X80 Laser Welded Joints,” pp. 1–19.